

X-Ray Characteristics of the Hot Stars in Trumpler 14 and 16

Kati Bilty & Nathan Miller
Department of Physics and Astronomy
University of Wisconsin-Eau Claire



Abstract

We have obtained X-ray data from the orbiting Chandra X-ray observatory in order to investigate the hot stars in the star clusters Trumpler 14 and 16. Our data set contains a number of CCD images centered on two stars in the clusters (HD93250 and HD93129). After combining our images into a master image, a major initial task was determining which sources were detected and identifying them with previously cataloged optical sources. The dimmest sources have resulted in only a handful of photon counts and are therefore at the edge of detection for the instrument, making these detections difficult. The images of the brightest stars have resulted in thousands of photon counts.

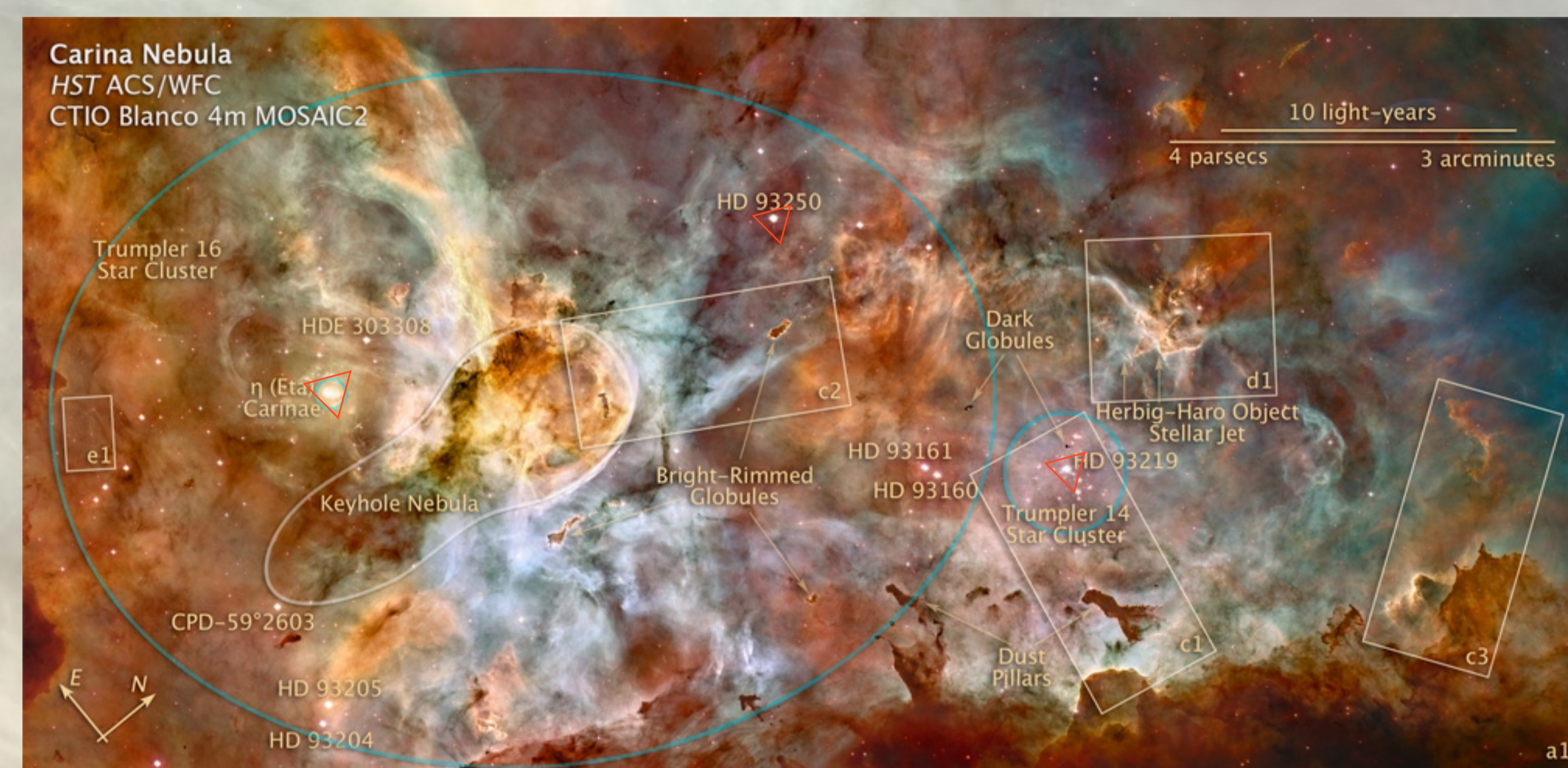


Figure 1 - This is a Hubble image of the Carina Nebula, NGC 3372. The Trumpler 14 star cluster can be seen on the right side of the image with its main star HD93129. This star, along with the star HD93250, which can be seen near the top of the image, are the two stars main stars the X-ray telescope was pointed at when our data was taken. The star Eta Carinae is on the left side of the image. The Trumpler 16 star cluster is on the left hand side of the image, and is much larger than the Trumpler 14 star cluster. (Image credit: NASA, ESA, N. Smith (U. California, Berkeley) et al., and The Hubble Heritage Team (STScI/AURA)).

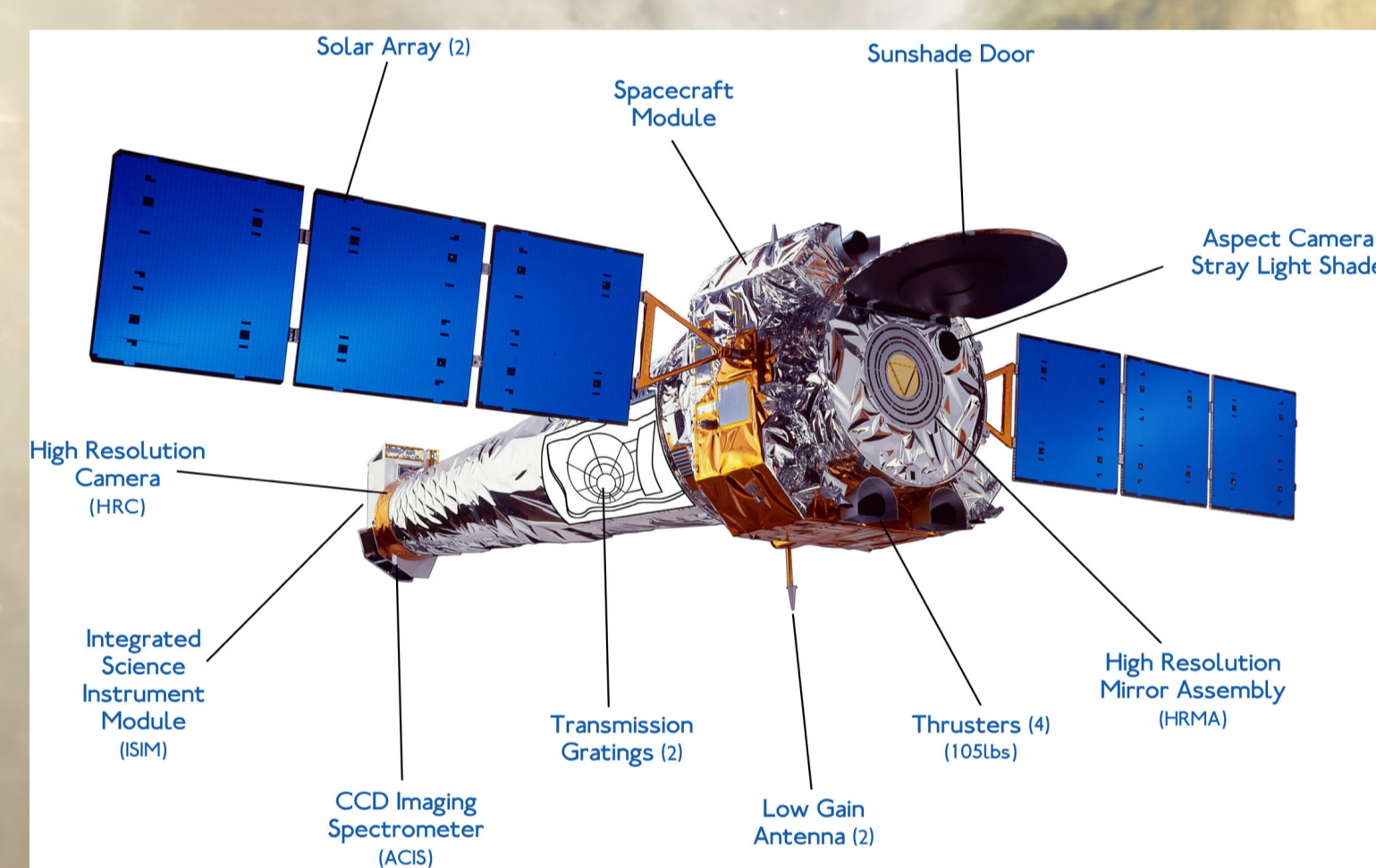


Figure 2 - The Chandra X-ray Observatory was launched July 23, 1999. Each image from Chandra has fifty times the resolution of the previous X-ray imaging instruments. After being taken, observational data is telemetered from orbit to Earth where it can be analyzed using the Chandra Interactive Analysis of Observations (CIAO) suite of programs which we have installed on the UWEC campus.

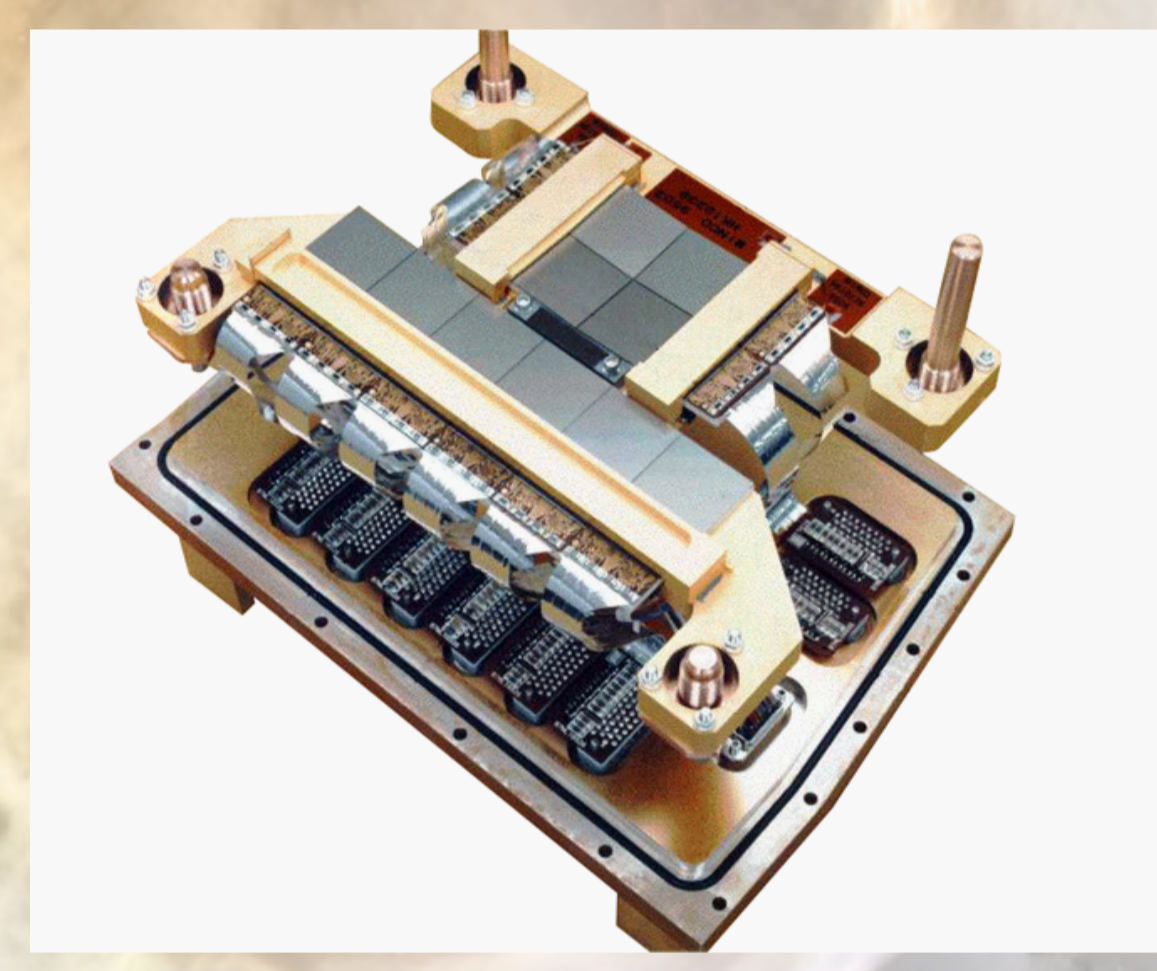


Figure 3 - The Advanced CCD Imaging Spectrometer, or ACIS, is made up of 10 CCD (or charge-coupled device) chips that take images and spectral data. When used in X-ray astronomy, there is one count per pixel for each photon that hits it. The resulting data can be used to make X-ray images and at the same time measures the energy of the X-ray. Appearing as dark squares in the above image, it can be seen that four of the chips form a square and the remaining six are in a linear array. During our observations only the six-element linear array was activated (ACIS-I).

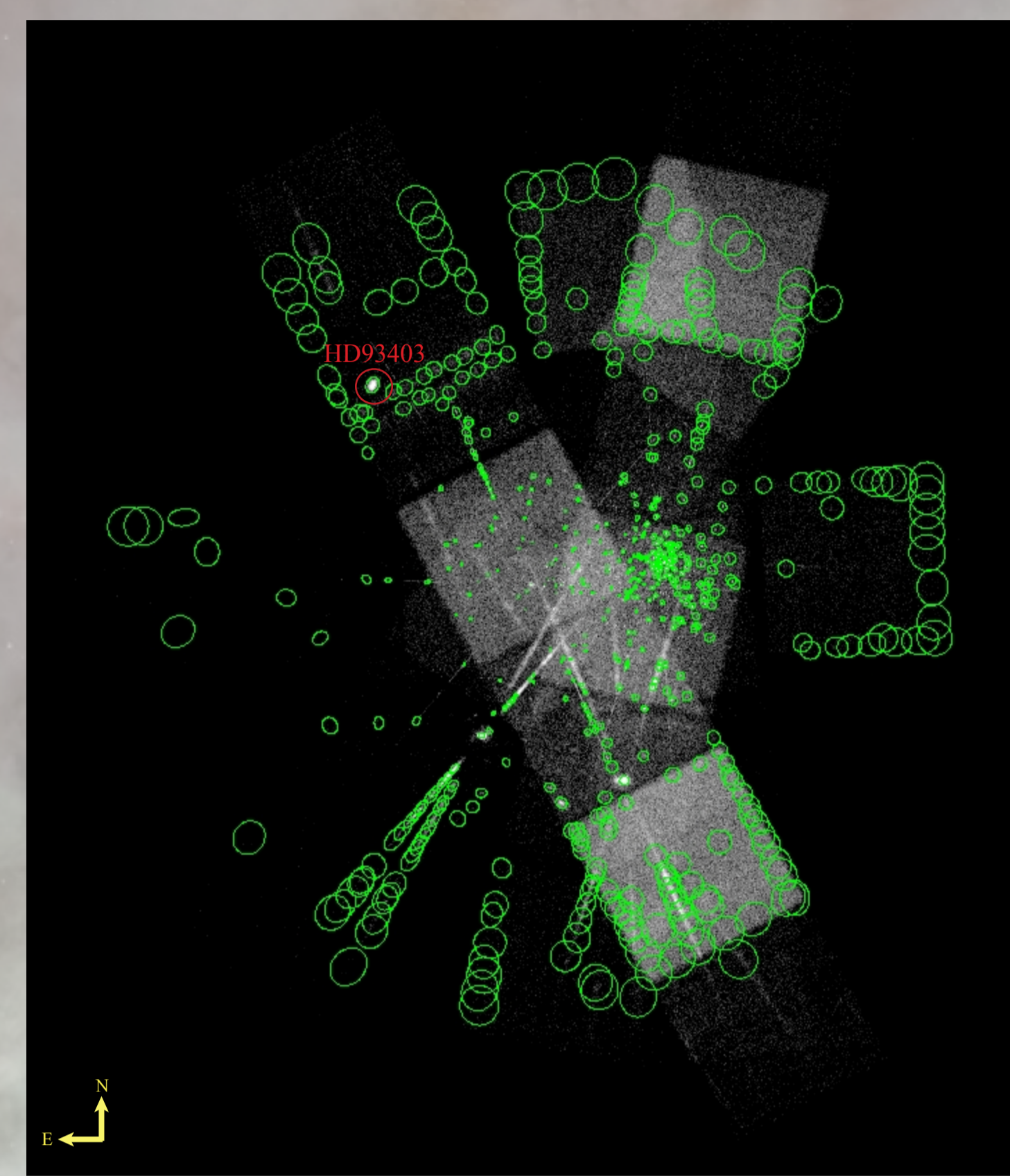


Figure 6 - The regions in this image were created using celldetect. Celldetect is a CIAO program that detects point sources within an exposure. The regions get larger the further they are from the axis because the uncertainty of the point source's position become larger. As can be seen in this figure, some detections are of false sources. The program compares the pixel counts to the background counts to find sources. Some of the false sources that celldetect identifies are caused by the edge of the detector and gaps between chips.

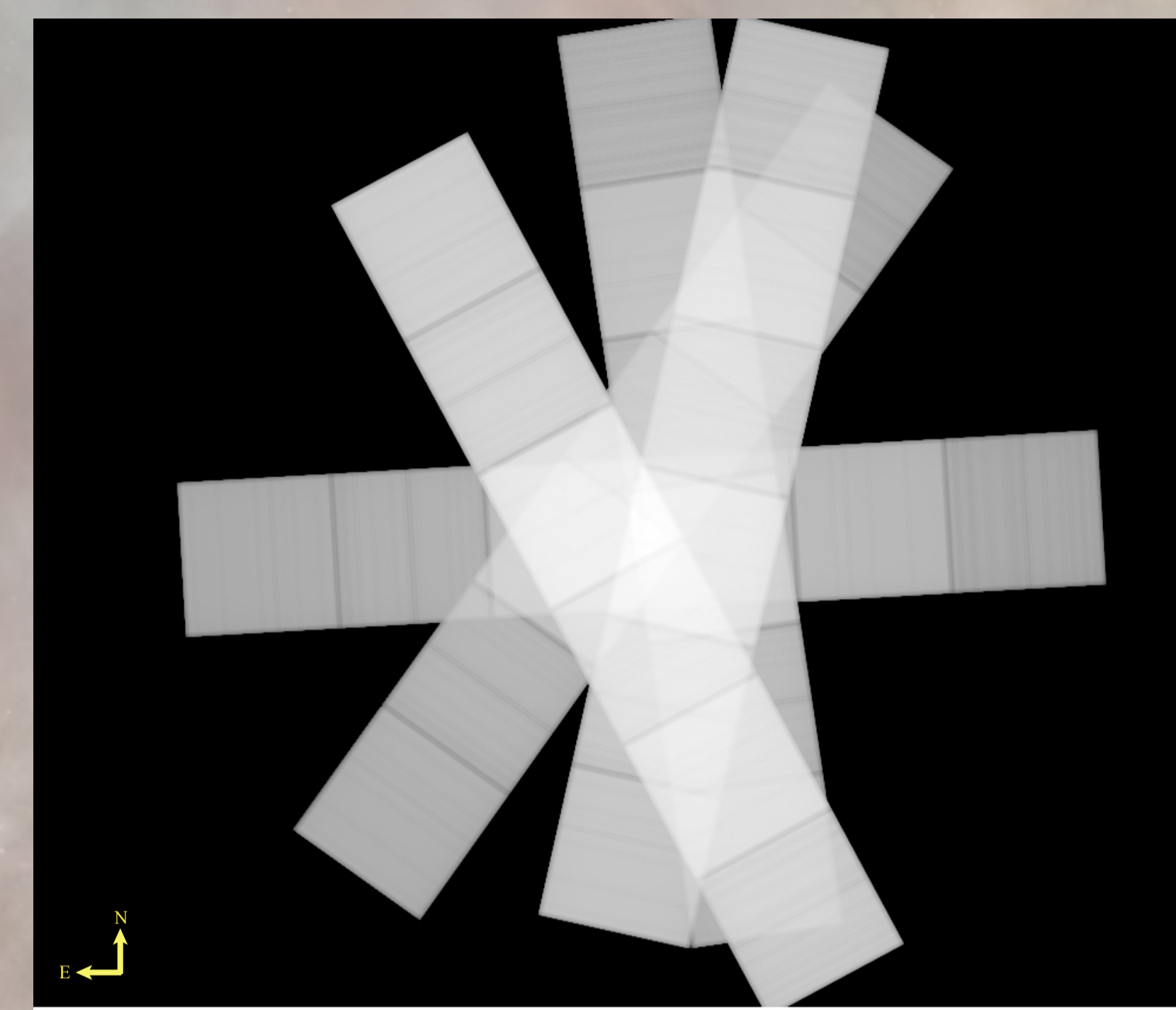


Figure 7 - This is an exposure map which we developed for the merged data. An exposure map displays the effective exposure time for each position on the sky - black indicates no exposure time and white indicates maximum exposure time. The blurring of the edges in this image is due to telescope dither. Dither evens out pixel-to-pixel inconsistencies and partially fill in the gaps between the chips by gently rocking the telescope through a complex pattern during the exposure. This exposure map was created to remove the detection of false sources when using celldetect. False sources can be caused by detector edges and chip gaps. In this case the exposure map is used with recursive blocking. Recursive blocking prevents a source at the edge of a chip from being detected twice.

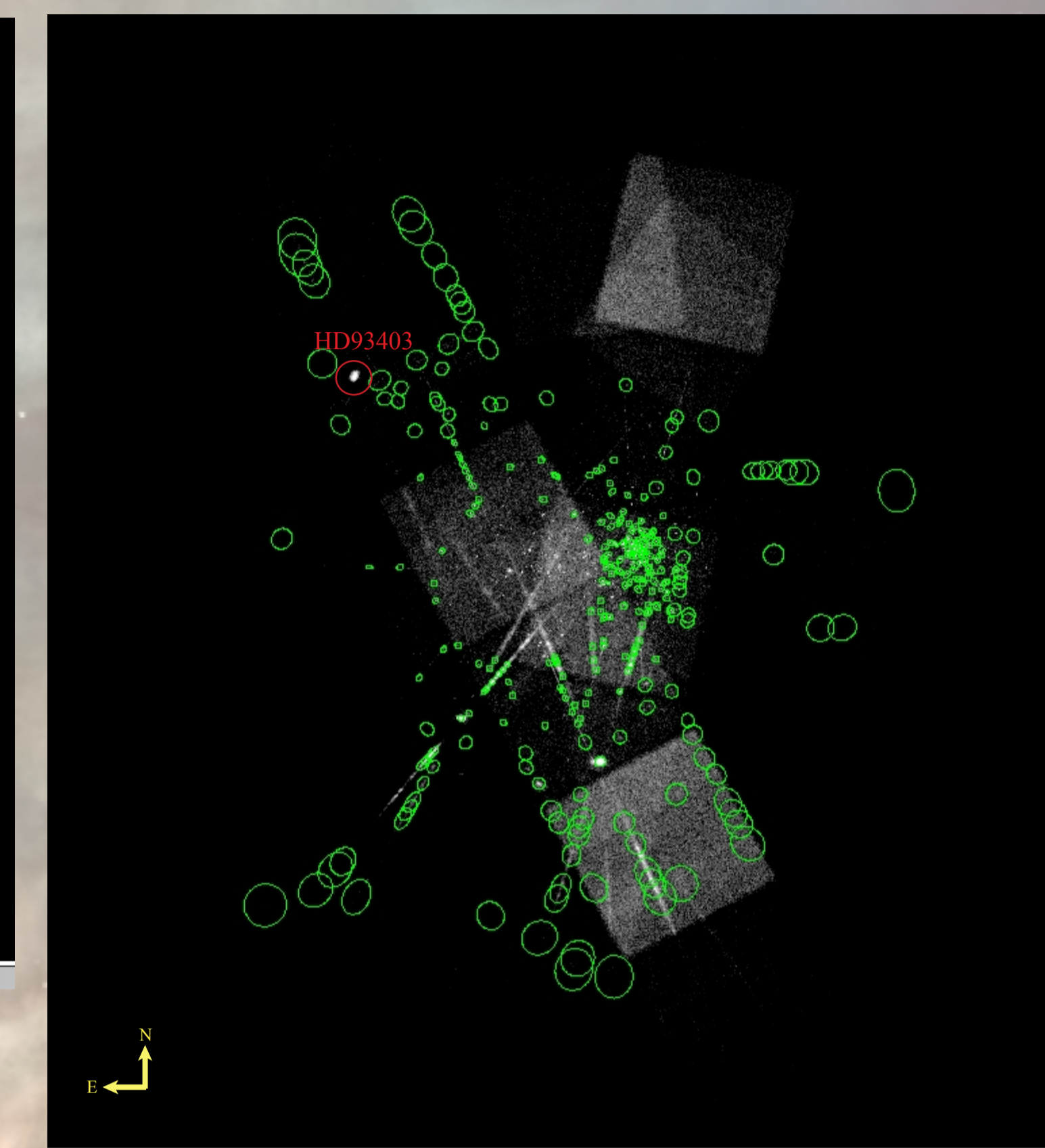


Figure 8 - This image shows how an exposure map eliminates false detections made by celldetect. Compared to Figure 6 this figure has fewer false sources. The red circle seen above is around a star that is not identified as a source by celldetect. We know this source to be the star HD93403 and it is one of the brightest sources in the above image. Celldetect labeled HD93403 as a point source before the exposure map was applied and can be seen in Figure 6. The brightness of the source may be the cause of its removal by the exposure map because the area may have been considered an area of "hot pixels." Hot pixels are individual pixels that look much brighter than they should.

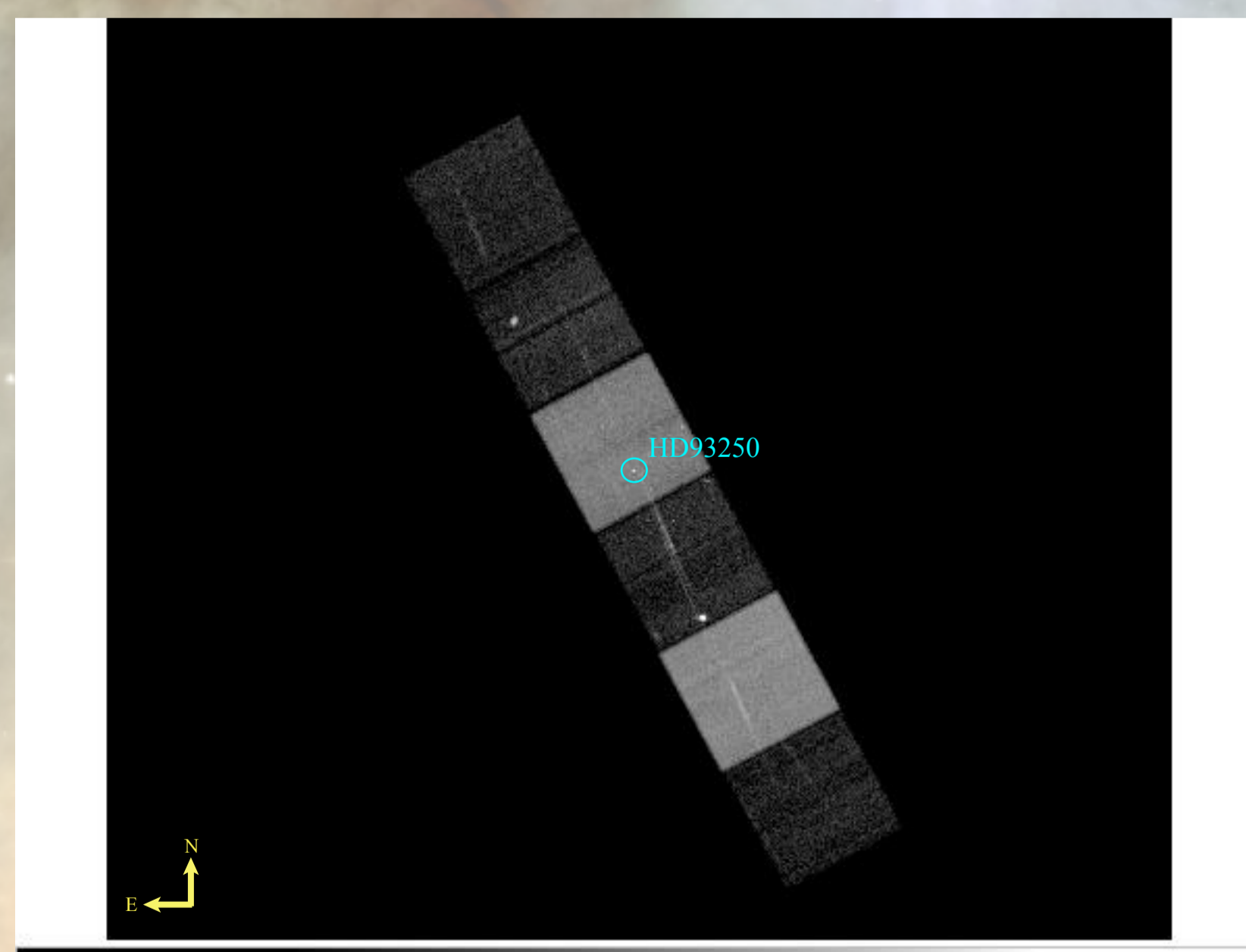


Figure 4 - This is a single X-ray image taken by the Chandra X-ray Observatory. The six chips of ACIS-I are visible (the different grey scales are due to their different characteristic background count rates). The star HD 93250 is in the center of this image. Each observation is given an observation ID (for example, this observation is ObsId 7341). There are a total of twelve observations in our data set. Each image is either centered on HD93250 or HD93129, which are both in the Carina Nebula.

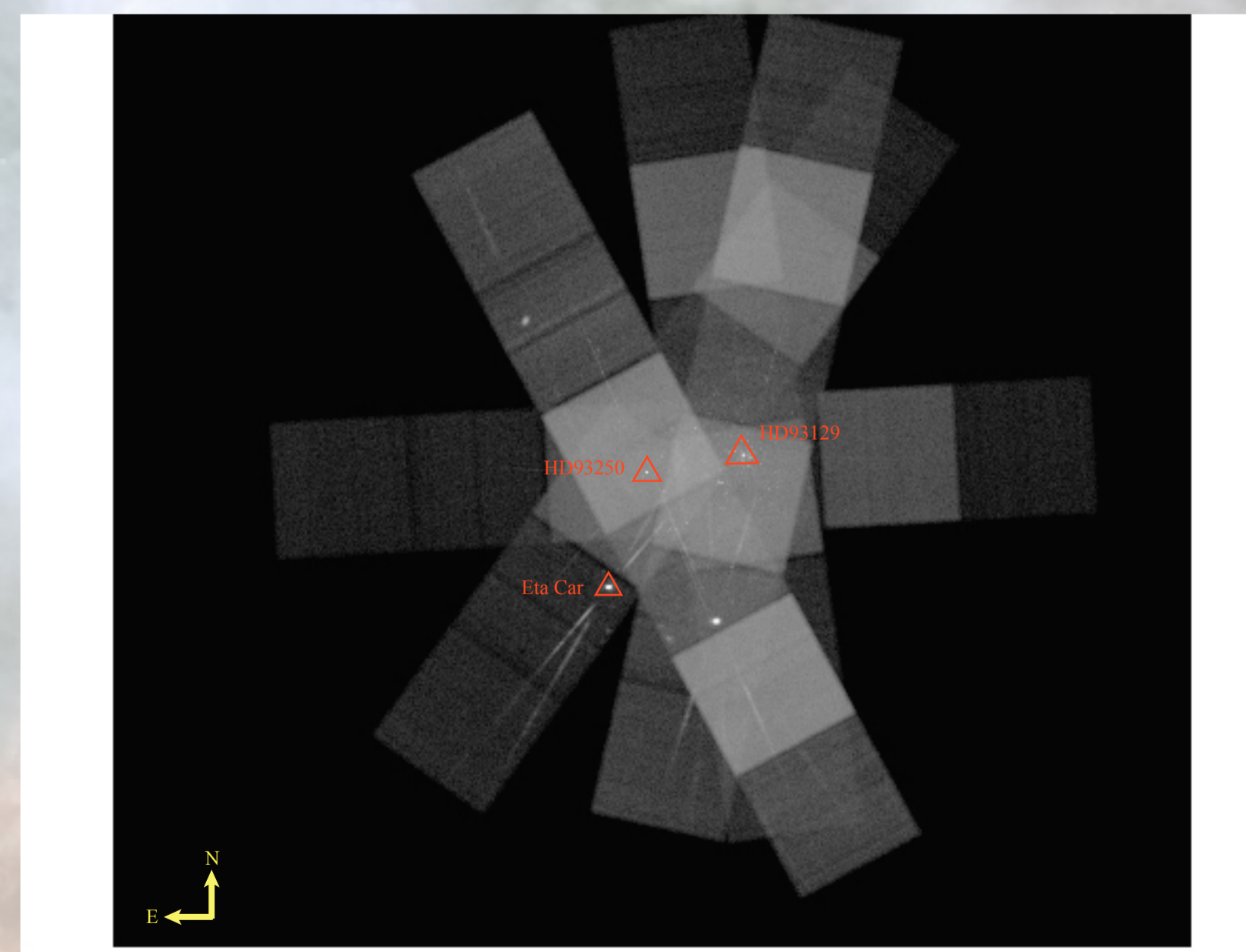


Figure 5 - The observations used were taken with different orientations, five observations targeted HD93250 while the other seven targeted HD93129. We merged all of the images to create a mosaic of the region. The different roll orientations of the CCD detector on the sky for the various exposures creates the asterisk-like pattern seen. The twelve observations were aligned using World Coordinate System, or WCS. Note that in this figure north is up. By comparing the positions of the stars HD93250, HD93129, and Eta Car it can be seen how this X-ray image relates to the visible image displayed in Figure 1.

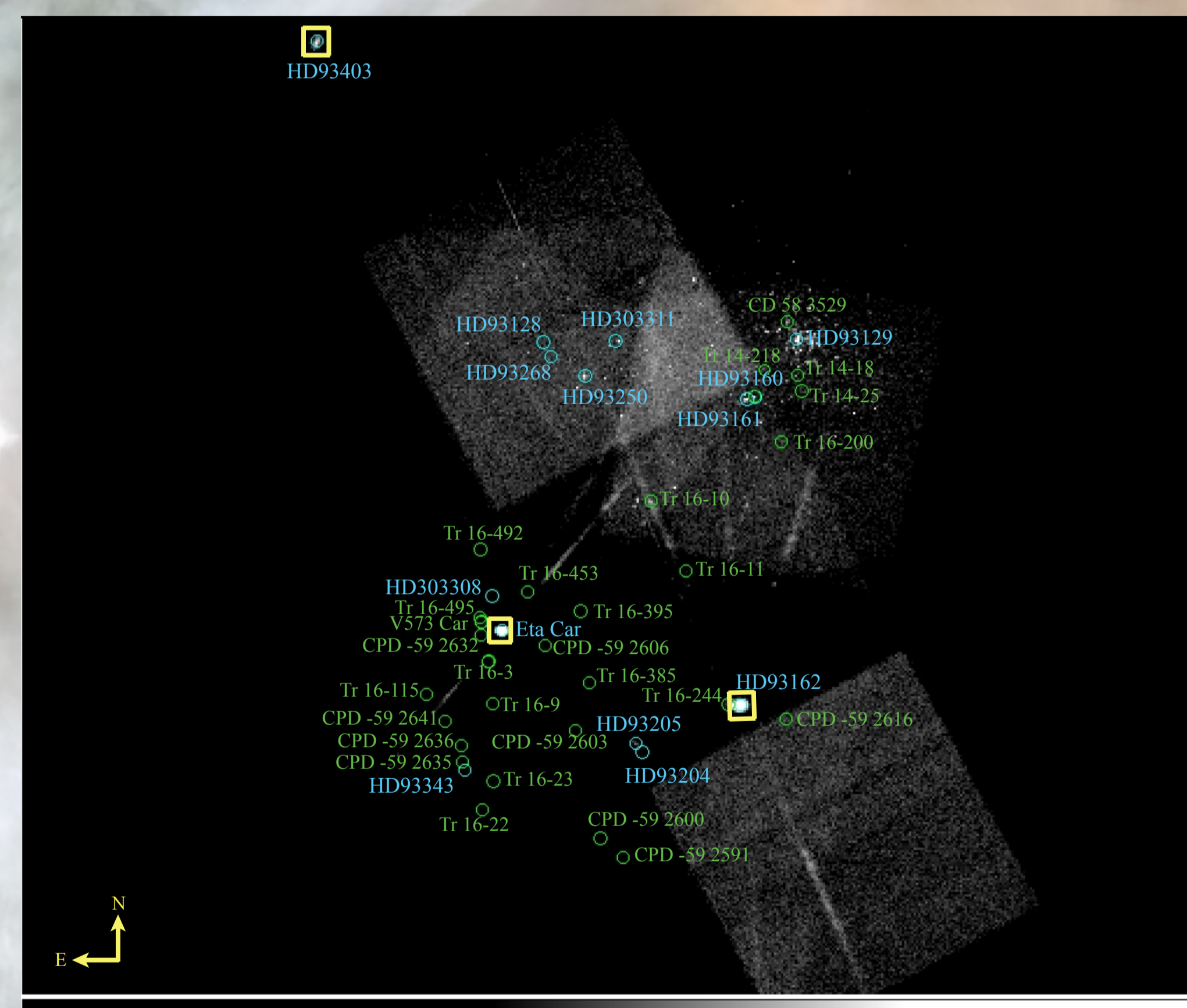


Figure 9 - This figure is an enlarged version of the center of Figure 5. After merging all of the data we identified the stars. Using Feinstein, Marraco, & Muzzio (1973) as our finder chart we were able to identify a handful of stars in our data. To find the exact coordinates of these stars we used SIMBAD, an online database of stars and their coordinates. The coordinates were then used to place region circles around the sources. The stars with blue regions and labels are the stars that were found in this manner. The stars with green regions and labels were found using a data table from Sanchawala et al (2007). This data table gave the coordinates of the stars which we then used to place the regions.

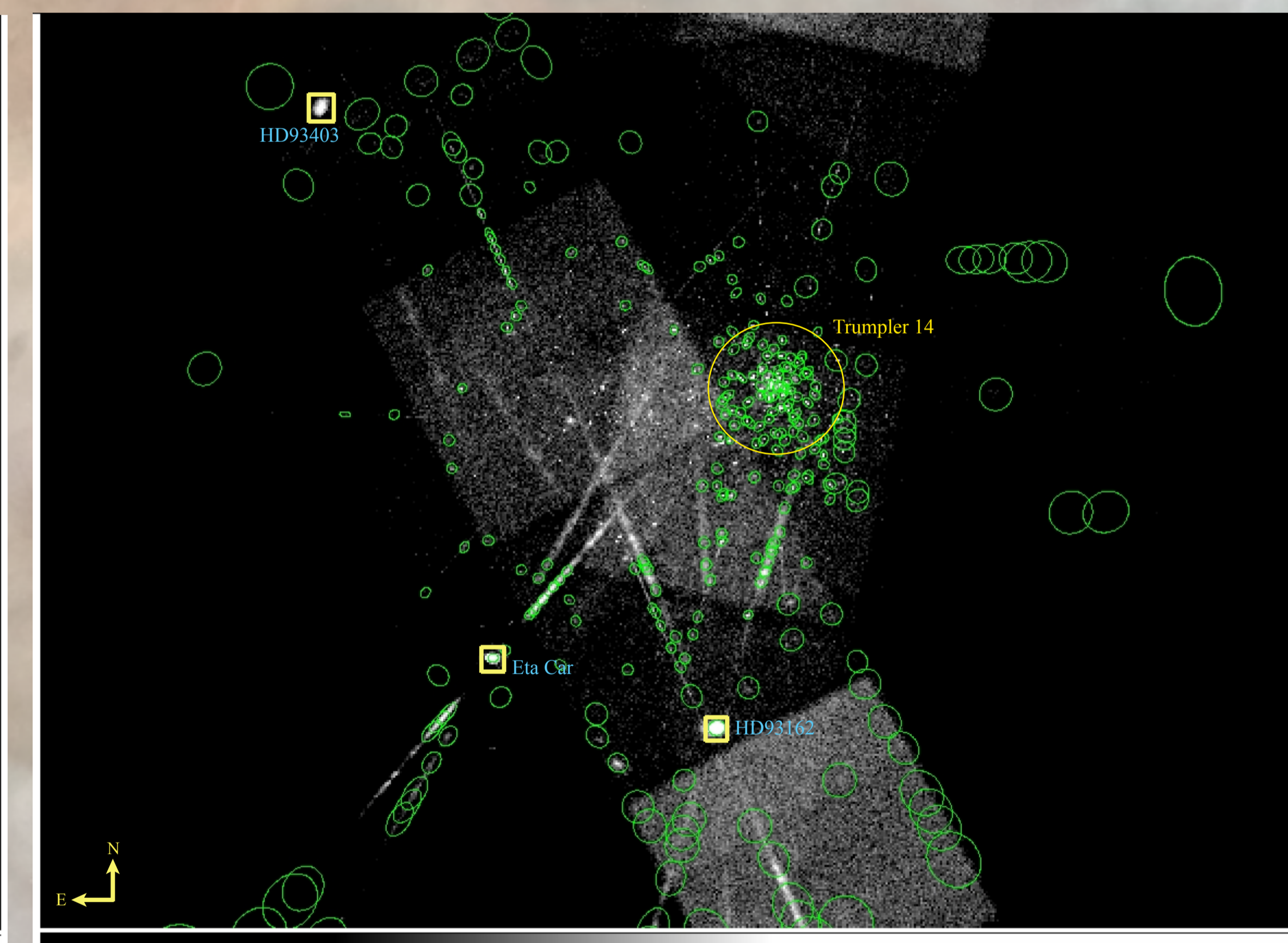


Figure 10 - This figure is an enlarged version of the center of Figure 8 (HD93403 are labeled in both for comparison). There are many more regions in this image compared to Figure 9 (HD93403, HD93162 and Eta Car are labeled in both images for comparison). Some of these regions may be false sources detected by celldetect, especially the regions along the edges of the CCD chips. In Trumpler 14 celldetect has identified a large number of sources. The yellow circle in the image shows the location of the Trumpler 14 star cluster. A large number of point sources found by celldetect in the Trumpler 14 region we have not yet identified. These are more difficult to identify because most sources do not have them all identified, for example, Sanchawala et al (2007) and Feinstein, Marraco, & Muzzio (1973) have not identified all sources in Trumpler 14 within their data.

Star	Spectral Type	Star	Spectral Type
HD 303308	O3 V	HD 93403	O6e
HD 93129	O3 lab	HD 93161	O6.5 V
HD 93205	O3.5 V	HD 93160	O6.5 V
HD 93128	O3.5 V	HD 93162	WN+
HD 93204	O5 V	Eta Car	LBV
HD 303311	O5 V	HD 93268	A2

Table 1 - In this table the stars in blue from Figure 9 are listed with their spectral type. O type stars are massive, bright, hot stars (they have the power of over a million times our sun) and are blue. The star HD93162 is a Wolf-Rayet star. These stars are supergiants with hot stellar winds that have blown away their outer layer leaving the hot helium shell. A type stars are one of the more common types of stars visible with the naked eye and are bluish-white (the well known stars Vega and Sirius are A type stars).